ACS APPLIED MATERIALS & INTERFACES

Research Article

www.acsami.org

Graphene-Based Hybrid Composites for Efficient Thermal Management of Electronic Devices

Michael Shtein,*[,†] Roey Nadiv,[‡] Matat Buzaglo,[‡] and Oren Regev*[,†,‡]

[†]Ilse Katz Institute for Nanoscale Science and Technology and [‡]Department of Chemical Engineering, Ben-Gurion University of the Negev, Beer-Sheva 8410501, Israel

Supporting Information

ABSTRACT: Thermal management has become a critical aspect in next-generation miniaturized electronic devices. Efficient heat dissipation reduces their operating temperatures and insures optimal performance, service life, and efficacy. Shielding against shocks, vibrations, and moisture is also imperative when the electronic circuits are located outdoors. Potting (or encapsulating) them in polymer-based composites with enhanced thermal conductivity (TC) may provide a solution for both thermal management and shielding challenges. In the current study, graphene is employed as a filler to fabricate composites with isotropic ultrahigh TC (>12 W m^{-1} K^{-1}) and good mechanical properties (>30 MPa flexural and compressive strength). To avoid short-circuiting the electronic assemblies, a dispersion of secondary ceramic-based filler reduces the electrical conductivity and synergistically enhances the TC of composites. When utilized as potting materials, these novel hybrid composites effectively dissipate the heat from electronic devices; their operating temperatures decrease from 110 to 37 °C, and their effective thermal resistances are drastically reduced, by up to 90%. The simple filler dispersion method and the precise manipulation of the composite transport properties via hybrid filling offer a universal approach to the large-scale production of novel materials for thermal management and other applications.

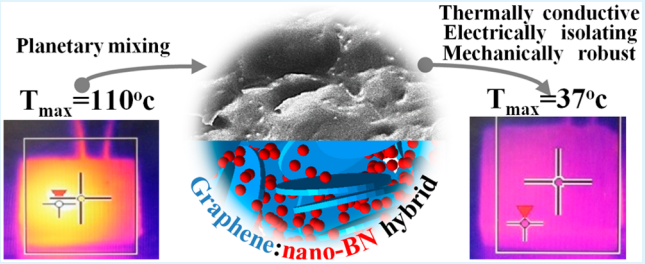

KEYWORDS: *graphene, boron nitride, hybrid nanocomposites, thermal conductivity, heat dissipation, potting*

INTRODUCTION

The denser and faster components of next-generation miniaturized electronics,[1−3] optoelectronics, and medical devices produce an increased amount of heat during their operation (>5 W cm^{-2}).[4] Without efficient thermal management, heat accumulation may damage these devices or severely reduce their speed, efficiency, and reliability.[5] Conventional heat removal solutions (e.g., by fans or metal heat sinks) may solve the heat accumulation challenge, but do not provide shielding against shock, vibration, moisture, and corrosive agents for electronic devices located outdoors.

Potting[6,7] or conformal coating of these electronic assemblies in a polymer-based composite with enhanced thermal conductivity (TC) may provide a solution for both thermal management and shielding challenges. Traditionally, the target TC values (>1 W m^{-1} K^{-1}) were met by dispersing high loadings[8,9] (50−80 vol %) of thermally conductive (TC = 30−300 W m^{-1} K^{-1}) fillers in thermally isolating polymers (TC < 0.3 W m^{-1} K^{-1}[10]). To avoid short-circuiting the electronic components, only electrically isolating ceramic-based fillers, such as SiC,[11,12] AlN,[6,13] BN,[6,7] or Al_2O_3,[14] were utilized. BN is considered the most efficient, due to its wide band gap (ranging from 3.6 to 7.1 eV[15]), low thermal expansion coefficient, and high moisture resistance. High loading and high filler densities, however, result in heavy weights and expensive composites with poor mechanical properties (e.g., susceptible to thermal cracking and complicated processing), the combination of which limit their applications.

In recent years, the growing availability of nanoscale carbon fillers with extraordinary thermal properties and low densities (e.g., graphene with TC = ∼5000 W m^{-1} K^{-1}[16] and ρ = 1.2 g m^{-3}) have yielded lightweight composites with enhanced TC at low filler loading.[17,18] Unfortunately, carbon-based fillers are electrically conductive (>10^7 S cm^{-1}). If the filler loading exceeds the percolation threshold, it also significantly increases the electrical conductivity (EC) of some potting composite materials (EC > 10^{-3} S cm^{-1}[19−22]) and short-circuits the electronic assemblies. A possible solution to this phenomenon is the loading of a secondary filler (termed "hybrid filler loading"). The hybrid loading was previously shown to synergistically increase the TC of composites,[17,23−25] and, as we recently demonstrated, if the secondary filler is electrically insulating, the hybrid loading may also significantly decrease their EC.[26]

In the current study, optimized hybrid composites with ultrahigh isotropic TC, low EC, and good mechanical properties are fabricated by means of a facile and scalable method. When utilized as potting materials, these hybrid

Received: August 24, 2015
Accepted: October 7, 2015
Published: October 7, 2015

DOI: 10.1021/acsami.5b07866
ACS Appl. Mater. Interfaces 2015, 7, 23725−23730

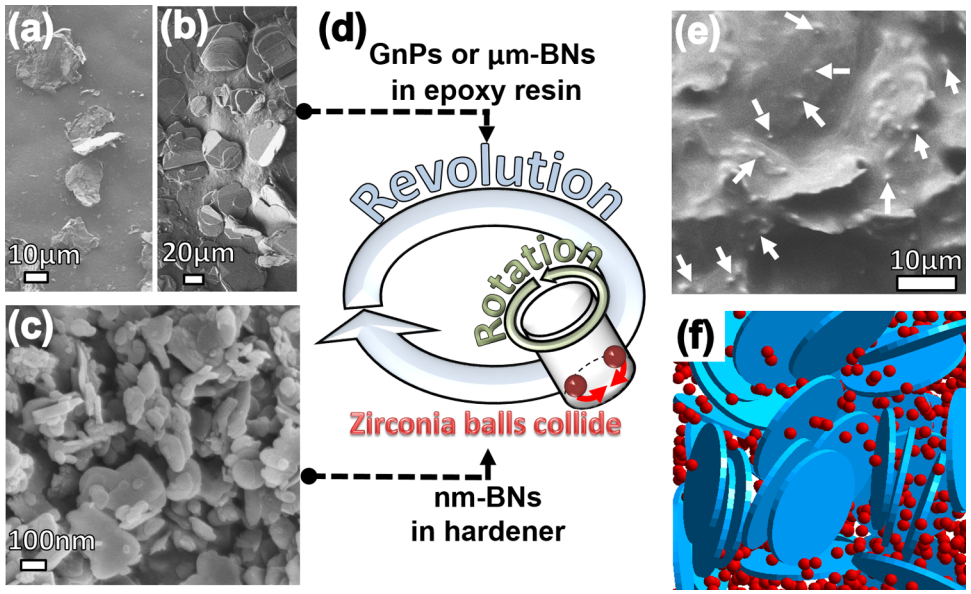

Figure 1. SEM micrographs of (a) graphene (GnPs), (b) μm-BN platelets, and (c) nm-BN spheres. (d) Schematics of the planetary dispersion process, assisted by zirconia balls to increase the compression forces (see Composite Preparation in the Experimental Section). (e) SEM micrograph of a fractured hybrid composite. The nm-BN spheres (marked with white arrows) are homogeneously dispersed between the GnPs. (f) Schematics of a hybrid composite. The blue platelets and red spheres indicate GnP/μm-BN and nm-BN, respectively.

composites effectively dissipate the heat generated in electronic devices and drastically reduce their maximal operating temperatures.

EXPERIMENTAL SECTION

Materials. Graphene nanoplatelets (GnPs with 15 μm lateral size and 10 nm thickness; XG-Sciences), micrometer-sized boron-nitride platelets (μm-BNs, 110 μm lateral size and 50 nm thickness; Advanced Ceramics), boron-nitride nanoparticles (nm-BNs, 110 nm; Hongwu), bisphenol A diglycidyl ether (EPON 828; Momentive), polyether triamine hardener (JEFFAMINE T-403; Momentive), 3-(glycidoxypropyl)trimethoxysilane (silane, Acros), pluronic F-127 (F-127, Sigma-Aldrich), and commercial potting material (CM,50−3182 NC, epoxies) were used as received.

Composite Preparation. Fillers in either an epoxy resin or a hardener (1 g of epoxy resin to 0.38 g of hardener) are added to a planetary centrifugal mixer (Thinky, ARE-310[27]). Zirconia balls measuring 5 mm were placed into the mixing container. The materials are mixed for 10 min at 2000 rpm and deaerated for 5 min at 2200 rpm. Then, the zirconia balls are removed and the composites are cast into silicone molds, shaped as detailed in corresponding ASTMs, and cured for 12 h at 80 °C. During the mixing process, the combination of rotational and revolving motions (Figure 1d) generates a spiral flow, along with rising and falling convection currents. The planetary motion also throws the zirconia balls strongly against each other, generating high impact energy and compresses the adjacent fillers, to form a denser filler network with lower phonon scattering.[26,28] In contrast to other dispersion methods, the planetary mixer is an extremely effective method for dispersing high filler loadings. The lack of mechanical blades eliminates the entrapment of air, thereby producing air-free composites with homogeneous filler dispersions. It is easily scalable up to 20 L,[29] which is highly significant for future large-scale production and the commercialization of these composites.

Composite Characterization. *Thermal conductivity* of bulk samples was measured using differential scanning calorimetry[30] (section 1.1 in the Supporting Information) or the transient plane heat source method (ISO 22007-2). *Electrical conductivity* measurements were conducted using a four-probe configuration on square-shaped samples (10 × 10 × 1 mm^3). *Mechanical properties* of the hybrid composites are determined by measuring at least seven duplicates by Instron 5982. The sample size and test conditions were adjusted according to ASTM D790 (flexural strength test) and ASTM D695 (compressive strength test). A high-resolution, cold, field emission gun scanning electron microscope (SEM, JSM-7400F, JEOL) was used to determine the lateral dimensions of the fillers and their dispersion in the epoxy matrix.

Thermal Management. Silicon carbide Schottky diodes (D06S60) were mounted on FR4 printed circuit boards and potted by a 4 mm thick composite layer. The diodes' power dissipation was kept constant (power = 2 W) by a Keithley 2400 SourceMeter. The operating temperatures of the devices were monitored by a FLIR E60 thermal camera and the local hotspot ($T_{hotspot}$) by a type K thermocouple. At least three heating (20 min)−cooling (160 min) cycles were monitored.

RESULTS AND DISCUSSION

First, a facile and scalable filler dispersion method is presented. Then, the effect of hybrid filler loading on thermal, electrical, and mechanical properties of polymer-based composites is evaluated. A demonstration of heat dissipation efficiency of optimized hybrid composites concludes this work.

Manufacturing of Composites. Thermally conductive graphene or BN nanoplatelets (GnPs or μm-BNs, Figure 1a,b), with micrometer-size lateral dimensions and nanosize thicknesses, were dispersed in an insulating epoxy resin in a planetary mixer with zirconia balls (Figure 1d and Experimental Section). The high rotational and revolving motions applied a powerful acceleration force that generated strong material convection, while zirconia balls significantly increased the compression and shear forces applied on the fillers. When coupled with optimized filler surface treatment (Supporting Information section 2.3), this scalable mixing technique resulted in air-free composites with well-dispersed filler.[26] In the hybrid composites, the *secondary* filler (spherical nanosize BN, nm-BN in Figure 1c) was dispersed in the epoxy hardener and then homogeneously integrated between the platelets (Figure 1e), during epoxy resin and hardener mixing. An optimal *primary-to-secondary* filler ratio (μm-BN:nm-BN or GnP:nm-BN, vide infra) was found to promote a platelet−

DOI: 10.1021/acsami.5b07866
ACS Appl. Mater. Interfaces 2015, 7, 23725−23730

sphere network (schematically depicted in Figure 1f) with an increased number of thermally conductive pathways.

Filler Effect on the TC, EC, and Mechanical Properties of Composites. The electrical and the thermal conductivities of the fillers (Table 1) dictated whether both composite transport properties were enhanced, or just the TC (Figure 2).

Table 1. TC and EC of Selected Materials[a]

	EC (S cm^{-1})	TC (W m^{-1} K^{-1})
GnP	**>10**[7][31]	**~2000−5300**[32]
boron nitride	<10^{-8}[33]	**>300**[34]
epoxy	10^{-16}	0.19

[a]Dominant properties are marked in bold.

Boron-Nitride-Based Composites. Electrically insulating composites were prepared by the integration of μm-BN platelets into the epoxy matrix. The TC of these composites increased significantly from 0.18 to 2.9 W m^{-1} K^{-1} (at filler volume fraction of φ = 0.44, Figure 2a), corresponding to a thermal conductivity enhancement factor (TCEF = (TC enhancement %)/(filler vol %)) of 36. This TCEF is comparable to the TCEF achieved by complex multistep dispersion methods[35−37] and substantially surpasses the TCEF values (=10) attained by other simple one-step mixing techniques.[38] As expected, the EC of BN-based composites remains unaltered (empty circles in Figure 2a), similar to the values of a neat polymer matrix.

Graphene-Based Composites. The utilization of GnPs as a filler results in thermally and electrically conductive materials (squares in Figure 2a), due to the GnPs' extraordinary electric and thermal conductance (Table 1). An isotropic ultrahigh TC of 12.4 W m^{-1} K^{-1} is achieved at φ_{GnP} = 0.24 and corresponds to a remarkable TCEF of 283. In contrast to the gradual increase in TC, the EC of GnP-based composites increases abruptly (by ~16 orders of magnitude, Figure 2a), which is in good agreement with previous reports.[19] Consequently, potting electronic devices within these electrically conductive composites will short-circuit, overheat, and damage them.

Thermal Percolation Thresholds. Interestingly, thermal percolation thresholds were observed in both the GnP- and μm-BN-based composites at φ = 0.17 (red arrows in Figure 2a). These thermal percolation values are comparable to the calculated geometrical percolation thresholds ($0.10 < \varphi_c < 0.27$) in systems with isotropically oriented, impermeable platelets with high aspect ratios (>50 and >1000 for graphene and BN platelets used in this study).[39,40] Below the percolation thresholds, the polymer mediates between adjacent platelets and the TC in this region is in excellent agreement with Nan's model[41] (eq S2 in the Supporting Information and the dotted lines in Figure 2a), assuming that high interfacial thermal resistance exists between the thermally conductive fillers, homogeneously dispersed in the insulating matrix. Above the threshold, the sharp rise in TC indicates that a 3-D network, with an increased number of direct platelet-to-platelet contacts and decreased polymer-mediated boundaries, has formed. The adjacent platelets (GnP or μm-BN) are pressed together during mixing by the zirconia balls (Figure 1d), closing the gaps between them to form a denser network with lower phonon scattering.[26] The TC in this region obeys the adjusted critical power law (eq S3 in the Supporting Information and the full lines in Figure 2a).[42]

Effects of Filler Size on TC. TC suppression with decreasing filler lateral size (i.e., increased interface densities) was observed in both BN- and GnP-based composites (Figure S3 in the Supporting Information), which may be explained by the diffuse surface scattering of heat carriers.[43,44] Accordingly, the hybrid composites were loaded by *primary* fillers with largest lateral dimensions (110 μm BNs and 15 μm GnPs).

Hybrid Composites. The EC and the TC of composites were further tuned by controlling the concentration of the *secondary* filler. The electrically insulating and thermally conductive nm-BNs were homogeneously dispersed (Figure 1e) together with GnPs or μm-BNs. To maximize the TC, while attaining the electrical and mechanical properties required for potting applications, we optimized the total filler loading, the *primary-to-secondary* filler ratio (Figure S4 in the Supporting Information), and the filler surface treatment (Figure S5 in the Supporting Information). The TC of the optimized hybrids is enhanced (by 72% for BN-based hybrid$_1$ and by 22% for GnP-based hybrid$_2$, Figure 2b) compared to single filled composites, suggesting a genuine synergistic effect. The nm-BN particles (red spheres in Figure 1f) dispersed between the platelets (blue disks in Figure 1f) increased the thermal coupling between them, on one hand, and acted as electrical insulators to drastically reduce the EC of the GnP-based composites (diamonds in Figure 2b), on the other. Both hybrid systems (Table 2) show good mechanical properties (>30 MPa flexural

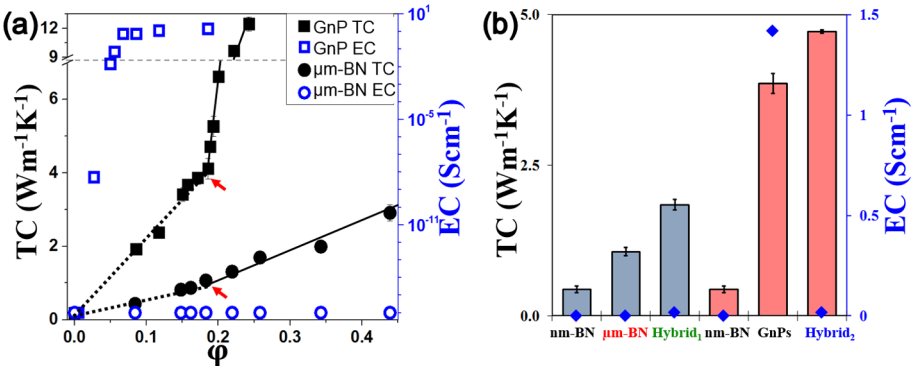

Figure 2. (a) TC and EC of composites as a function of filler type and volume fraction (φ). The dotted and full lines are fits to the Nan's (eq S2) and adjusted percolation (eq S3) models, respectively. The slopes' intersections (marked by red arrows) reveal the thermal percolation thresholds. (b) TC of composites with total filler loading of φ = 0.17: Hybrid$_1$ composite filled with $\varphi_{\mu m\text{-}BN}$ = 0.15 and $\varphi_{nm\text{-}BN}$ = 0.02; hybrid$_2$ composite filled with $\varphi_{nm\text{-}GnP}$ = 0.16 and $\varphi_{nm\text{-}BN}$ = 0.01. Note that some error bars assimilated into the markers, due to the small measurement errors.

DOI: 10.1021/acsami.5b07866
ACS Appl. Mater. Interfaces 2015, 7, 23725−23730

Table 2. Properties of Hybrid and Commercially Available Potting Materials

	filler type	φ	TC (W m^{-1} K^{-1})	flexural strength (MPa)	compressive strength (MPa)	EC (S cm^{-1})	density (g cm^{-3})	workability
commercial material[45]	BN	0.80	1.66	65	90	4.9×10^{-16}	2.3	poor
hybrid$_1$	μm-BN	0.15	1.84 ± 0.10	42 ± 1	108 ± 3	5.0×10^{-16}	1.2	good
	nm-BN	0.02						
hybrid$_2$	GnP	0.16	4.72 ± 0.10	32 ± 2	60 ± 3	4.0×10^{-15}	1.1	good
	nm-BN	0.01						

and compressive strength), comparable to commercial potting materials[45] but with increased TC, significantly lower filler loading (0.80 vs 0.17) and density, and enhanced workability.

Thermal Management. Heat dissipation efficiency was evaluated by potting an electronic device (e.g., diode in Figure 3a,b and Experimental Section) in the electrically insulating and

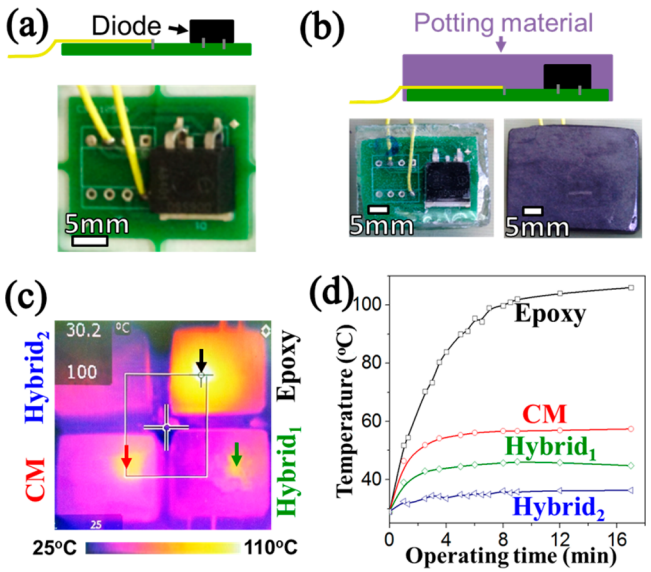

Figure 3. Photographs and schematics of: (a) an electronic device, (b) electronic devices potted in thermally insulated epoxy matrix (bottom left), and thermally conductive hybrid$_2$ (bottom right; the composition is detailed in Table 2). (c) Thermal micrograph of electronic circuits potted by neat epoxy (upper right), commercial thermal material (bottom left), hybrid$_1$ (bottom right), and hybrid$_2$ (upper left) composites after 10 min of operation. Arrows indicate hotspot regions. (d) Maximum temperatures ($T_{hotspot}$) of the electronic circuits as a function of their operation time. Note the error bars assimilated into the markers, due to the small measurement errors.

thermally conductive hybrid composites and monitoring the temperatures via thermal imaging (Figure 3c and Figure S6 in the Supporting Information). The operating temperatures of the devices were recorded as a function of their operating times (Figure 3d), and the effective thermal resistances were calculated as follows:[46,47]

$$\theta_{eff} = (T_{hotspot} - T_{ambient})/\text{power} \quad (1)$$

where $T_{hotspot}$ is the maximal temperature (usually near the diode's surface) at steady operating conditions, $T_{ambient}$ is the temperature of the surrounding environment (27 °C), and power is the electric power consumption of the electronic device.

Potting the electronic device in a thermally insulating epoxy matrix (0.19 W m^{-1} K^{-1}) demonstrated extremely high θ_{eff} (48 K W^{-1}), manifested by significant heat accumulation near the heat-emitting diode, with a 110 °C "hotspot" (region where the local temperature is significantly higher than the average temperature, marked by a black arrow in Figure 3c). The highly loaded (φ_{BN} = 0.80) commercial material (CM) produced only slight heat dissipation efficiency, with a 55 °C hotspot (marked by red arrow) and θ_{eff} of 18 K W^{-1}. In comparison, the hybrid$_1$ composite (μm-BN:nm-BN), with its significantly lower loading (φ = 0.17), achieved superior thermal management (θ_{eff} = 10 K W^{-1} and 45 °C hotspot, marked by green arrow). Finally, encapsulating the electronic circuit within a highly thermally conductive and electrically isolating hybrid$_2$ composite (GNP:nm-BN) reduced the device's operating temperature notably from 110 to 37 °C and its θ_{eff} by 90% (from 48 to 5 K W^{-1}). Remarkably, the hotspot was practically eliminated (Figure S6 in the Supporting Information) as predicted by recently published numerical studies.[48,49] The attained low and uniform temperature profile across the devise ensures its enhanced service life and efficacy.

CONCLUSIONS

A scalable and facile dispersion method was utilized to fabricate composites with ultrahigh thermal conductivity, low electrical conductivity, and good mechanical properties at low filler loading. Control over the transport properties was achieved by forming a hybrid 3-D network incorporating nm-BN with μm-BN or GnP. The secondary filler (nm-BN) increased the amount of thermally conductive pathways, on one hand, and disconnected the electrically conductive network, on the other. Therefore, when utilized as a potting material, these hybrid composites effectively dissipate the heat from electronic devices and drastically reduce their operating temperatures (from 110 to 37 °C), while providing shielding against external shock and vibration. The suggested, simple dispersion method and the accurate control of composite transport properties offer a universal approach to the large-scale production of new composites for future thermal management applications.

ASSOCIATED CONTENT

Supporting Information

The Supporting Information is available free of charge on the ACS Publications website at DOI: 10.1021/acsami.5b07866.

Thermal conductivity determination and models, effects of filler size, primary-to-secondary filler ratio, and fillers surface treatment on TC of composites, and heat dissipation efficiency (PDF)

AUTHOR INFORMATION

Corresponding Authors

*(M.S.) E-mail: shteinm@gmail.com.
*(O.R.) E-mail: oregev@bgu.ac.il.

Notes

The authors declare no competing financial interest.

DOI: 10.1021/acsami.5b07866
ACS Appl. Mater. Interfaces 2015, 7, 23725−23730

ABBREVIATIONS

EC = electrical conductivity
CM = commercial potting material
GnPs = graphene nanoplatelets
nm-BNs = boron-nitride nanoparticles
TC = thermal conductivity
μm-BNs = micrometer-sized boron-nitride platelets

REFERENCES

(1) Viswanath, R.; Wakharkar, V.; Watwe, A.; Lebonheur, V. Thermal Performance Challenges from Silicon to Systems. *Intel Technol. J.* **2000**, *Q3*, 1−16.
(2) Yim, M. J.; Paik, K. W. Recent Advances on Anisotropic Conductive Adhesives (ACAs) for Flat Panel Displays and Semiconductor Packaging Applications. *Int. J. Adhes. Adhes.* **2006**, *26*, 304−313.
(3) Moore, G. E. Cramming More Components onto Integrated Circuits, Reprinted from Electronics, Volume 38, Number 8, April 19, 1965, pp.114 ff. *Solid-State Circuits Newsl., IEEE* **2006**, *11*, 33−35.
(4) HCL Technologies, Thermal Management in Electronic Equipment, http://www.hcltech.com/sites/default/files/Thermal_Management_in_Electronic_Equipment_01FEB10_V1.pdf, accessed: August, 2015.
(5) Moore, A. L.; Shi, L. Emerging Challenges and Materials for Thermal Management of Electronics. *Mater. Today* **2014**, *17*, 163−174.
(6) Zhu, B. L.; Ma, J.; Wu, J.; Yung, K. C.; Xie, C. S. Study on the Properties of the Epoxy-matrix Composites Filled with Thermally Conductive AlN and BN Ceramic Particles. *J. Appl. Polym. Sci.* **2010**, *118*, 2754−2764.
(7) Li, T. L.; Hsu, S. L. C. Enhanced Thermal Conductivity of Polyimide Films via a Hybrid of Micro- and Nano-Sized Boron Nitride. *J. Phys. Chem. B* **2010**, *114*, 6825−6829.
(8) Pierson, H. O. *Handbook of Carbon, Graphite, Diamond and Fullerenes: Properties, Processing and Applications*; Noyes Publications: Park Ridge, NJ, USA, 1993.
(9) Wypych, G. *Handbook of Fillers: Physical Properties of Fillers and Filled Materials*; ChemTec Publishing, Toronto, Canada, 2010.
(10) Han, Z.; Fina, A. Thermal Conductivity of Carbon Nanotubes and their Polymer Nanocomposites: A review. *Prog. Polym. Sci.* **2011**, *36*, 914−944.
(11) Lee, G.-W.; Park, M.; Kim, J.; Lee, J. I.; Yoon, H. G. Enhanced Thermal Conductivity of Polymer Composites Filled with Hybrid Filler. *Composites, Part A* **2006**, *37*, 727−734.
(12) Yang, K.; Gu, M. Enhanced Thermal Conductivity of Epoxy Nanocomposites Filled with Hybrid Filler System of Triethylenetetramine-Functionalized Multi-Walled Carbon Nanotube/Silane-Modified Nano-sized Silicon Carbide. *Composites, Part A* **2010**, *41*, 215−221.
(13) Jiajun, W.; Xiao-Su, Y. Effects of Interfacial Thermal Barrier Resistance and Particle Shape and Size on the Thermal Conductivity of AlN/PI Composites. *Compos. Sci. Technol.* **2004**, *64*, 1623−1628.
(14) Fu, J.; Shi, L.; Zhang, D.; Zhong, Q.; Chen, Y. Effect of Nanoparticles on the Performance of Thermally Conductive Epoxy Adhesives. *Polym. Eng. Sci.* **2010**, *50*, 1809−1819.
(15) Watanabe, K.; Taniguchi, T.; Kanda, H. Direct-bandgap Properties and Evidence for Ultraviolet Lasing of Hexagonal Boron Nitride Single Crystal. *Nat. Mater.* **2004**, *3*, 404−409.
(16) Balandin, A. A.; Ghosh, S.; Bao, W. Z.; Calizo, I.; Teweldebrhan, D.; Miao, F.; Lau, C. N. Superior Thermal Conductivity of Single-Layer Graphene. *Nano Lett.* **2008**, *8*, 902−907.
(17) Shahil, K. M. F.; Balandin, A. A. Graphene−Multilayer Graphene Nanocomposites as Highly Efficient Thermal Interface Materials. *Nano Lett.* **2012**, *12*, 861−867.
(18) Du, F.-p.; Yang, W.; Zhang, F.; Tang, C.-Y.; Liu, S.-p.; Yin, L.; Law, W.-C. Enhancing the Heat Transfer Efficiency in Graphene−Epoxy Nanocomposites Using a Magnesium Oxide−Graphene Hybrid Structure. *ACS Appl. Mater. Interfaces* **2015**, *7*, 14397−14403.
(19) Xiang, J.; Drzal, L. T. Investigation of Exfoliated Graphite Nanoplatelets (xGnP) in Improving Thermal Conductivity of Paraffin Wax-Based Phase Change Material. *Sol. Energy Mater. Sol. Cells* **2011**, *95*, 1811−1818.
(20) Stankovich, S.; Dikin, D. A.; Dommett, G. H. B.; Kohlhaas, K. M.; Zimney, E. J.; Stach, E. A.; Piner, R. D.; Nguyen, S. T.; Ruoff, R. S. Graphene-Based Composite Materials. *Nature* **2006**, *442*, 282−286.
(21) Fu, X.; Yao, C.; Yang, G. Recent Advances in Graphene/Polyamide 6 Composites: a Review. *RSC Adv.* **2015**, *5*, 61688−61702.
(22) Liang, J.; Wang, Y.; Huang, Y.; Ma, Y.; Liu, Z.; Cai, J.; Zhang, C.; Gao, H.; Chen, Y. Electromagnetic Interference Shielding of Graphene/Epoxy Composites. *Carbon* **2009**, *47*, 922−925.
(23) Goyal, V.; Balandin, A. A. Thermal properties of the Hybrid Graphene-Metal Nano-Micro-Composites: Applications in Thermal Interface Materials. *Appl. Phys. Lett.* **2012**, *100*, 073113.
(24) Renteria, J.; Legedza, S.; Salgado, R.; Balandin, M. P.; Ramirez, S.; Saadah, M.; Kargar, F.; Balandin, A. A. Magnetically-Functionalized Self-Aligning Graphene Fillers for High-Efficiency Thermal Management Applications. *Mater. Des.* **2015**, *88*, 214−221.
(25) Goli, P.; Ning, H.; Li, X.; Lu, C. Y.; Novoselov, K. S.; Balandin, A. A. Thermal Properties of Graphene−Copper−Graphene Heterogeneous Films. *Nano Lett.* **2014**, *14*, 1497−1503.
(26) Shtein, M.; Nadiv, R.; Buzaglo, M.; Kahil, K.; Regev, O. Thermally Conductive Graphene-Polymer Composites: Size, Percolation, and Synergy Effects. *Chem. Mater.* **2015**, *27* (6), 2100−2106.
(27) *Thinky ARE-310*, http://www.thinkyusa.com/products/item-all/rotation-revolution-mixer/are-310.html, accessed August 2015.
(28) Mio, H.; Kano, J.; Saito, F.; Kaneko, K. Effects of rotational direction and rotation-to-revolution speed ratio in planetary ball milling. *Mater. Sci. Eng., A* **2002**, *332*, 75−80.
(29) *Thinky ARV-10kTWIN*, http://www.thinkyusa.com/products/item-all/vacuum-mixer/arv-10ktwin.html. accessed August 2015.
(30) Mettler Toledo. *Simple Determination of the Thermal Conductivity of Polymers by DSC*, http://sg.mt.com/sg/en/home/supportive_content/matchar_apps/MatChar_UC226.html, accessed August 2015.
(31) *Stream, Graphene Nanoplatelets Data*, http://www.strem.com/uploads/resources/documents/graphene_nanoplatelets.pdf, accessed August, 2015.
(32) Balandin, A. A. Thermal properties of Graphene and Nanostructured Carbon Materials. *Nat. Mater.* **2011**, *10*, 569−581.
(33) Nose, K.; Oba, H.; Yoshida, T. Electric Conductivity of Boron Nitride Thin Films Enhanced by in Situ Doping of Zinc. *Appl. Phys. Lett.* **2006**, *89*, 112124.
(34) Jo, I.; Pettes, M. T.; Kim, J.; Watanabe, K.; Taniguchi, T.; Yao, Z.; Shi, L. Thermal Conductivity and Phonon Transport in Suspended Few-Layer Hexagonal Boron Nitride. *Nano Lett.* **2013**, *13*, 550−554.
(35) Wang, Z.; Fu, Y.; Meng, W.; Zhi, C. Solvent-Free Fabrication of Thermally Conductive Insulating Epoxy Composites with Boron Nitride Nanoplatelets as Fillers. *Nanoscale Res. Lett.* **2014**, *9*, 643−643.
(36) Kim, K.; Kim, J. Fabrication of Thermally Conductive Composite With Surface Modified Boron Nitride by Epoxy Wetting Method. *Ceram. Int.* **2014**, *40*, 5181−5189.
(37) Kim, K.; Kim, M.; Hwang, Y.; Kim, J. Chemically Modified Boron Nitride-Epoxy Terminated Dimethylsiloxane Composite for Improving the Thermal Conductivity. *Ceram. Int.* **2014**, *40*, 2047−2056.
(38) Gu, J.; Zhang, Q.; Dang, J.; Xie, C. Thermal Conductivity Epoxy Resin Composites Filled with Boron Nitride. *Polym. Adv. Technol.* **2012**, *23*, 1025−1028.
(39) Chatterjee, A. P. Percolation Thresholds for Polydisperse Circular Disks: a Lattice-Based Exploration. *J. Chem. Phys.* **2014**, *141*, 034903.
(40) Otten, R. H. J.; van der Schoot, P. Connectivity Percolation of Polydisperse Anisotropic Nanofillers. *J. Chem. Phys.* **2011**, *134*, 094902.
(41) Nan, C.-W.; Liu, G.; Lin, Y.; Li, M. Interface Effect on Thermal Conductivity of Carbon Nanotube Composites. *Appl. Phys. Lett.* **2004**, *85*, 3549−3551.

DOI: 10.1021/acsami.5b07866
ACS Appl. Mater. Interfaces 2015, 7, 23725−23730

(42) Bonnet, P.; Sireude, D.; Garnier, B.; Chauvet, O. Thermal Properties and Percolation in Carbon Nanotube-Polymer Composites. *Appl. Phys. Lett.* **2007**, *91*, 201910.
(43) Chatterjee, S.; Nafezarefi, F.; Tai, N. H.; Schlagenhauf, L.; Nuesch, F. A.; Chu, B. T. T. Size and Synergy Effects of Nanofiller Hybrids Including Graphene Nanoplatelets and Carbon Nanotubes in Mechanical Properties of Epoxy Composites. *Carbon* **2012**, *50*, 5380−5386.
(44) Ziman, J. M. *Electrons and Phonons: The Theory of Transport Phenomena in Solids*; Oxford University Press: Oxford, U.K., 1960.
(45) *Epoxies, Thermally Conductive Epoxy Resin Data*, http://www.epoxies.com/_resources/common/userfiles/file/50-3182NC.pdf, accessed August 2015.
(46) Cengel, Y.; Ghajar, A. *Heat and Mass Transfer: Fundamentals and Applications*; McGraw-Hill Education: New York, 2010.
(47) Edwards, D. *Semiconductor and IC Package Thermal Metrics Texas Instruments 2012*, http://www.ti.com/lit/an/spra953b/spra953b.pdf, accessed August 2015.
(48) Hajmohammadi, M. R.; Salimpour, M. R.; Saber, M.; Campo, A. Detailed Analysis for the Cooling Performance Enhancement of a Heat Source Under a Thick Plate. *Energy Convers. Manage.* **2013**, *76*, 691−700.
(49) Hajmohammadi, M. R.; Moulod, M.; Shariatzadeh, O. J.; Campo, A. Effects of a Thick Plate on the Excess Temperature of Iso-Heat Flux Heat Sources Cooled by Laminar Forced Convection Flow: Conjugate Analysis. *Numer. Heat Transfer, Part A* **2014**, *66*, 205−216.

DOI: 10.1021/acsami.5b07866
ACS Appl. Mater. Interfaces 2015, 7, 23725−23730